Observation of granularity in YNi_2B_2C superconductors containing normal impurity phases

E. Bar-Sadeh, I. Felner, U. Asaf, and O. Millo*
Racah Institute of Physics, The Hebrew University, Jerusalem 91904, Israel
(Received 11 April 1995)

Cryogenic scanning tunneling microscopy is used to study the local electronic properties of intermetallic YNi_2B_2C superconductors. Samples which were prepared with Ni deficiency showed a sharp superconducting transition, onset around 15 K, while x-ray-diffraction measurements clearly indicated a presence of a nonsuperconducting YB_2C_2 phase. Our scanning tunneling spectroscopy measurements on these samples show strong spatial variations of the tunneling conductance, consistent with granular materials. In particular, we observe reproducible transitions between normal regions to superconducting regions, having a gap parameter of 2.55 ± 0.05 meV at 4.2 K, on length scales of 20 nm. In addition, the *I-V* characteristics often manifest single-electron tunneling effects, also typical of granular systems.

INTRODUCTION

The interest in intermetallic superconductors has been recently increased after the discovery of superconductivity in quaternary intermetallic compounds RNi_2B_2C, where R standing for rare earth or Y.[1] The highest transition temperatures, $T_c = 15.6$ and 16.6 K, were observed for single-phase compounds with R =Y and Lu, respectively. Studies performed on these boride-carbide compounds indicate that they conform closely to conventional type-II superconductors in the weak-coupling regime. These studies include characterization of the magnetic properties[2] and tunneling measurements[3,4] of the superconducting energy gap 2Δ. The origin of the relatively high-T_c in these materials, however, is not yet fully understood. The RNi_2B_2C compounds were found to crystallize in a tetragonal layered structure, with alternating Ni_2B_2 and RC layers.[1,5] It has been suggested that the low mass of boron, together with the strong Ni-B bonds in the Ni_2B_2 planes, yield high phonon frequencies and consequently a high T_c. It is not known yet whether this layered structure leads to gap anisotropy, as observed[6] for the layered high-T_c cuprates.

The boride-carbide superconductors are prepared by first melting Ni-rich high-purity constituents in Ar atmosphere, followed with an annealing step.[1-4] The melts are always found to contain a significant nonsuperconducting impurity phase. Only after an annealing one obtains nearly single-phase polycrystalline material, with less than 2% impurity phase. A study of the physical properties of Y-Ni-B-C systems containing a significant amount of a normal (nonsuperconducting) phase has not been reported yet. From the applied point of view, such studies may shed light on the processes taking place during the annealing stage and thus yield information that might help to achieve the goal of growing RNi_2B_2C single crystals. From the more fundamental point of view, one can learn about the physical properties of systems consisting of a *disordered* arrangement of normal and superconducting domains. Somewhat related to this subject is the problem of superconductivity in the high-T_c cuprates, which can be described as *ordered* arrays of discrete superconducting layers, separated by normal or insulating layers, and coupled by Josephson interaction.[7,8]

In this paper we present a cryogenic scanning tunneling microscopy (CSTM) study of YNi_2B_2C samples which contain about 20% of a nonsuperconducting impurity phase, identified from x-ray-diffraction pattern as YB_2C_2. The main goal of this paper is to characterize *locally* the electronic properties of this disordered normal-superconductor system. Our spatially resolved tunneling-spectroscopic data show surprisingly rapid and sharp transitions from fully superconducting to fully normal regions, which can be attributed to a granular normal-superconductor material, with weak coupling between neighboring grains. Moreover, the tunneling current-voltage (*I-V*) characteristics often exhibit single-electron tunneling (SET) effects,[9,10] such as the Coulomb blockade and the Coulomb staircase, consistent with the picture of weakly coupled grains.

EXPERIMENTAL

In order to ensure the presence of a significant nonsuperconducting phase we have prepared the samples by melting nonstoichiometric (but highly pure) elemental constituents, with some Ni *deficiency*. The melting was performed in an induction furnance in Ar atmosphere. The x-ray-diffraction pattern indicates that the major phase ($\sim$80%) consists of a body-centered-tetragonal structure with lattice parameters of $a = 3.53$ Å and $c = 10.55$ Å, corresponding to the YNi_2B_2C superconducting phase.[1] The pattern contains several impurity peaks corresponding to YB_2C_2 ($\sim$20%) and some other unidentified extra lines (less than 3%). No significant changes were observed, neither in the x-ray-diffraction pattern nor in the zero-field-cooling magnetization curve (see below), after annealing the ingot for 120 h at 950 °C. This indicates that the main source of the nonsuperconducting phase is not crystal defects, but rather the Ni deficiency, that cannot be removed by annealing. Figure 1 shows the temperature dependence of the magnetization, not corrected for a demagnetization factor, mea-

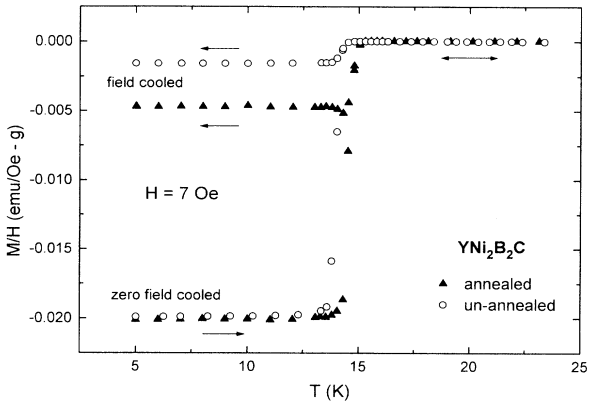

FIG. 1. Temperature dependence of the magnetization measured at a field $H=7$ Oe for two YNi_2B_2C samples, one annealed (solid triangles) and one unannealed (open circles). The arrows indicate the direction of thermal cycling for the measurements after zero-field cooling and for cooling in the presence of magnetic field.

sured for two samples, one before (open circles) and one after (solid triangles) annealing. The measurements were done in a field of 7 Oe, using a superconducting quantum interference device magnetometer (Quantum Design). The two magnetization traces are very similar in the zero-field-cooling part, and they both demonstrate a sharp superconducting transition. The transition is onset at 15.0 and at 14.8 K for the annealed and the unannealed sample, respectively. A real difference between the two traces can be observed *only* in the field cooling part, showing smaller flux expulsion for the unannealed sample. These results suggest that annealing was effective in reducing the density of flux-pinning centers, but left the volume fraction of the nonsuperconducting phase nearly intact.

Specimens were sliced from the ingot, and then polished first by fine Al_2O_3 powder and ending with 0.25 μm diamond lapping compound just before mounting in our homemade[10] CSTM. The STM was immersed in liquid He right after evacuating the sample space, and the sample and the scan head were cooled down to 4.2 K via He exchange gas. The STM topographic images were measured in the constant current mode, where a feedback circuit controls the tip-to-sample separation for a given setting of the tunneling current, I_S, and tip bias, V_S. The I-V curves, on the other hand, were acquired while momentarily *disconnecting* the feedback circuit. We note here that, while routinely achieving atomic resolution for highly oriented pyrolytic graphite surfaces with our CSTM, we could not obtain atomically resolved topographic images for the mechanically polished YNi_2B_2C surfaces.

RESULTS AND DISCUSSION

We present below only measurements performed on an unannealed sample; the results for the annealed samples were very similar. We first present and discuss typical I-V curves acquired in a region that exhibits superconductivity. (The spatial variations in superconductivity will be discussed below.) Shown in Fig. 2(a) are two tunneling I-V characteristics ("noisy" lines), taken at 4.2 K (lower curve) and at 8 K (upper curve). The tunneling-current and tip-bias settings (before disconnecting the feedback circuit) were different for the two curves: $I_S=1$ nA, $V_S=22$ mV, and $I_S=1$ nA, $V_S=15$ mV for the lower and the upper curve, respectively. These settings correspond to large-bias (compared to Δ) tunneling resistances $R_{nn}=22$ and 15 MΩ for the upper and the lower curve, respectively. Each experimental curve is plotted together with a theoretical curve (smooth line) calculated from the normal-insulator-superconductor (NIS) tunneling-junction model, as explained below. In Fig. 2(b) we plot the normalized tunneling conductance $G(V)/G_{nn}=(dI/dV)R_{nn}$, where $G_{nn}=1/R_{nn}$ is the large-bias tunneling conductance. These curves were calculated numerically from the corresponding I-V characteristics in Fig. 2(a). The normalized tunneling-conductance curves

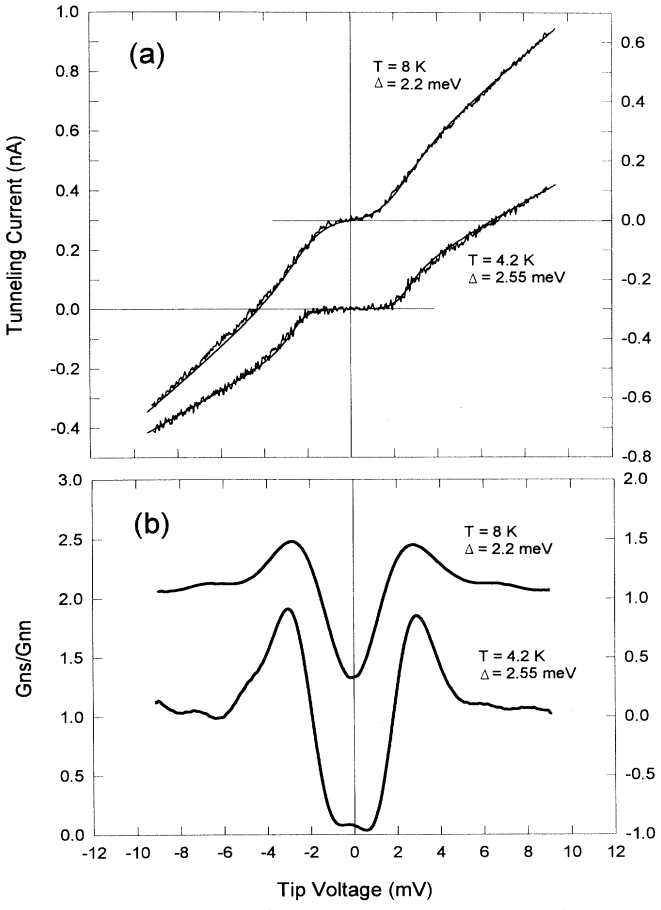

FIG. 2. (a) Two experimental tunneling I-V characteristics ("noisy" lines) measured at a superconducting region on the YNi_2B_2C surface. The lower curve was measured at 4.2 and the upper at 8 K. The solid lines were calculated from the NIS model with superconducting gap parameters of 2.55 and 2.2 meV, respectively. (b) Normalized conductance curves obtained numerically from the measured I-V characteristics.

depict the local tunneling density of states (DOS), in this case the superconductor quasiparticle DOS.

The two curves in Fig. 2(a) exhibit a pronounced gap structure (suppression of the tunneling-current) around zero bias, that can be associated with the superconducting energy gap of YNi_2B_2C, commonly observed in NIS tunnel junctions.[4,11,12] However, there are also other mechanisms that can yield gaps in the tunneling DOS, and thus gap structures in the I-V curves. One possibility is SET effects, such as the Coulomb blockade and the Coulomb staircase.[9,10,13–15] In order to distinguish experimentally between the I-V characteristics showing a superconducting gap and those manifesting SET effects, one can look at the effect of changing the STM setting (I_S and V_S) on the I-V curves. The I-V characteristics exhibiting SET effects depend strongly on this setting, both in the small-bias (tunneling gap) regime and in the large-bias regime,[9,10,13–15] as will be shown below. On the other hand, the superconducting energy gap, and thus the gap in the NIS tunnel-junction characteristics, are not sensitive to the STM setting. Changing this setting, however, will obviously be manifested in the large-bias tunneling conductance. When measuring the I-V traces in Figs. 2(a) and 3(a) we employed this procedure of changing the STM setting, and found no effect on the gap width for a wide range of tunneling resistances, $5\ \text{M}\Omega \le R_{nn} \le 60\ \text{M}\Omega$. In order to determine the local superconducting gap 2Δ, we fitted the finite-temperature BCS expression[11,12] for the tunneling current in NIS tunnel junction to our experimental data. The theoretical curves [smooth lines in Fig. 2(a)] were calculated with $\Delta = 2.55$ meV (for 4.2 K) and $\Delta = 2.20$ meV (for 8 K), as indicated in the figure, and are in excellent agreement with experiment. We want to emphasize that the fits were done using only one fitting parameter, Δ, as the value of R_{nn} is determined by the STM setting. The value of 2.55 (± 0.05) meV for Δ, with $T_c \approx 15$ K, gives the ratio $2\Delta/k_B T_c \approx 3.9$, which is somewhat larger than the BCS prediction for conventional superconductors, $2\Delta/k_B T_c = 3.53$. As the temperature is increased from 4.2 to 8 K, Δ decreases from 2.55 to 2.2 meV, consistent with the behavior of conventional superconductors. A more detailed study of the temperature and magnetic-field dependencies of Δ will be published elsewhere.

In what follows, we shall concentrate on the spatial variations of the tunneling conductance and on the granular properties of our YNi_2B_2C samples. The rapid spatial transition from superconducting-to-normal behavior is demonstrated by Fig. 3. Here we present two tunneling I-V characteristics measured at 4.2 K at different tip positions, about 30 nm apart. The positions are indicated on the STM topographic image, taken *simultaneously* with the I-V curves, using the settings of $I_S = 1$ nA and $V_S = 40$ mV. The two I-V curves, each typical for the region where it has been acquired, show qualitatively different behaviors. Curve (a) displays a clear superconductor-gap structure typical for NIS tunnel junctions, as discussed above. Curve (b), on the other hand, is purely ohmic, corresponding to a normal-insulator-normal tunnel junction with a tunneling resistance $R_{nn} \cong 40\ \text{M}\Omega$. Note that the tunneling resistance dV/dI in curve (a) approaches asymptotically the same value of $\sim 40\ \text{M}\Omega$ at bias voltages larger than the superconducting gap parameter, $\Delta \cong 2.55$ meV in this case. Focusing now on the topographic image, one can observe three distinct regions separated by clear boundaries: A relatively flat region at the right-hand side of the image, where I-V trace (a) was acquired, a steeply elevated area at the left-hand side, where I-V trace (b) was taken, and a small low plateau at the front corner. These regions will be denoted below as (a), (b), and (c), respectively. The topographic images were taken at a bias voltage much larger than Δ, thus the topographic images do not reflect changes in the local DOS, but rather correspond to the surface morphology of the YNi_2B_2C sample. This was further confirmed by the fact that the apparent barrier height,[16] extracted from current vs tip-sample separation measurements, was found to be nearly constant along the sample, ~ 2.8 eV.

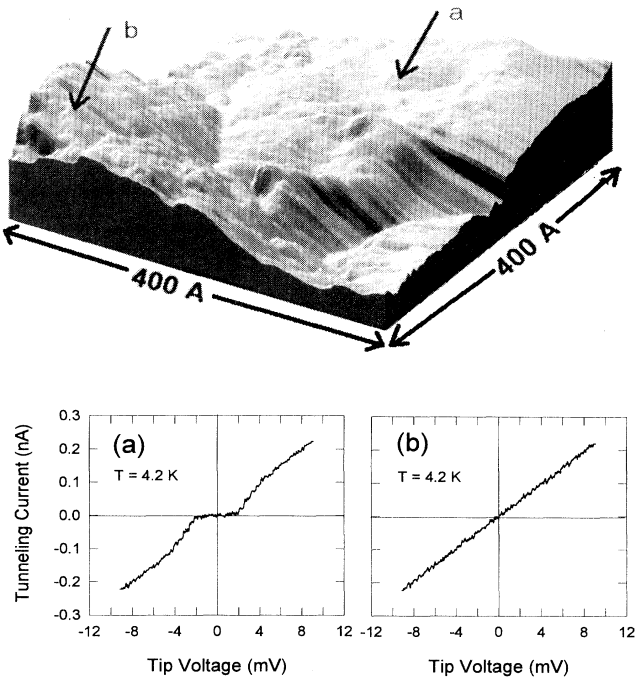

FIG. 3. Topographic image and two tunneling I-V characteristics of an YNi_2B_2C sample measured at 4.2 K. Curve (a) was measured in a superconducting region, while curve (b) in a normal region. The tip positions at which the curves were measured are indicated on the topographic image.

As already pointed out above, each of the two I-V curves in Fig. 3 is a typical representative of the I-V characteristics taken at the corresponding spatial region. [The characteristics measured at region (c) were ohmic, similar to those acquired at region (b).] The spatial transition from superconductivity to normal behavior occurred across the boundary, clearly observed in the topographic image, between regions (a) and (b). This was found to be a general behavior in our samples: the transi-

tions between areas exhibiting different tunneling-conductance properties (superconducting, normal, and SET effects) *always* took place across "topographic boundaries." Thus, our measurements show that the tunneling-conductance properties, in particular the variations in the surface-superconductivity, are correlated with the surface morphology of the YNi_2B_2C samples. This suggests that our samples consist of randomly dispersed superconducting (YNi_2B_2C) and normal (probably YB_2C_2) grains, and thus may be described as granular normal-superconductor systems. This picture is consistent with the x-ray-diffraction pattern. Spatial fluctuations in the surface superconductivity were also reported by de Lozanne, Elrod, and Quate[17] and Chang *et al.*[18] for Nb_3Sn and $Bi_2Sr_2CaCu_2O_8$ superconductors, respectively. These authors, however, have attributed the fluctuations to surface inhomogeneity, possibly caused by the damage created while preparing the surface for STM measurements.

The spatial transition from normal to superconducting regions commonly occurred over distances of ~ 20 nm. This value seems to be reasonable, since it is larger than, and therefore consistent with, the coherence length of YNi_2B_2C, ~ 10 nm.[2] However, it is still surprising that superconductivity was not induced in the normal regions by proximity effect.[12] We recall that the *I-V* characteristics taken at the normal region [Fig. 3(b)] were *purely ohmic,* showing no trace of a gap structure. The suppression of the proximity effect may be due to a weak coupling (large contact resistance) between the superconducting grains and the neighboring normal grains, at least in those places where a sharp spatial transition between superconducting to normal behavior is observed. Evidence for this weak-coupling, granular picture serves the observation that our *I-V* characteristics often exhibited SET effects, as will be discussed in the next paragraphs.

The quantized nature of the electrical charge significantly influences the electrical transport in systems composed of small metallic clusters. The tunneling probability in such systems may strongly depend on the electrostatic charging energy due to the addition of a *single* electron to a metal cluster. This leads to SET effects in the tunneling *I-V* characteristics such as the Coulomb blockade and Coulomb staircase.[9,10,13–15] The Coulomb blockade manifests itself by the suppression of the current around zero bias, while the Coulomb staircase exhibits a sequence of steps in the *I-V* curve. A widely studied structure that exhibits SET effects is the double-barrier tunnel junction geometry, where a small metal cluster is coupled via two tunnel junctions to two macroscopic electrodes.[9,13–15] If the *total* capacitance of the island with respect to its environment is small enough and if the resistance of *each* junction exceeds h/e^2, the Coulomb blockade can be observed experimentally. The width of the Coulomb blockade region depends on the effective fractional residual charge, Q_0, on the central electrode. When $Q_0=0$ the width is maximal, whereas for $Q_0=\pm e/2$ the Coulomb blockade is completely suppressed. For a highly asymmetric double-barrier tunnel junction a Coulomb staircase is observed, consisting of a series of equidistantly spaced steps in the *I-V* traces. Each step corresponds to the addition of a single electron to the center electrode. The value of Q_0 (mod e) can be obtained[13,14] from $Q_0=(C_1\Delta\phi_1-C_2\Delta\phi_2)/e$, where C_i and $\Delta\phi_i$ are the capacitances and work-function differences across junctions $i=1,2$. Thus, in a double-barrier tunnel junction realized in a STM experiment, where the tip serves as one of the macroscopic electrodes, the capacitance of the corresponding junction, and thus Q_0, can be changed *continuously* by varying the tip-cluster separation.

In Fig. 4 we present two experimental *I-V* traces ("noisy" lines) exhibiting SET effects. The two curves were measured *at the same lateral position,* on a surface-grain ~ 10 nm in diameter, but with different STM settings, and thus with *different tip-sample separations.* Curve (a) was measured with $I_S=1$ nA and $V_s=60$ mV, while curve (b) with $I_S=1.2$ nA and $V_S=60$ mV. Curve (a) displays both Coulomb blockade and a Coulomb staircase, whereas in curve (b) the Coulomb blockade is completely suppressed. These *I-V* characteristics, as well as the behavior upon changing the STM setting, are typical to the double-barrier tunnel junction configuration. We therefore conclude that the grain (~ 10 nm diameter) on

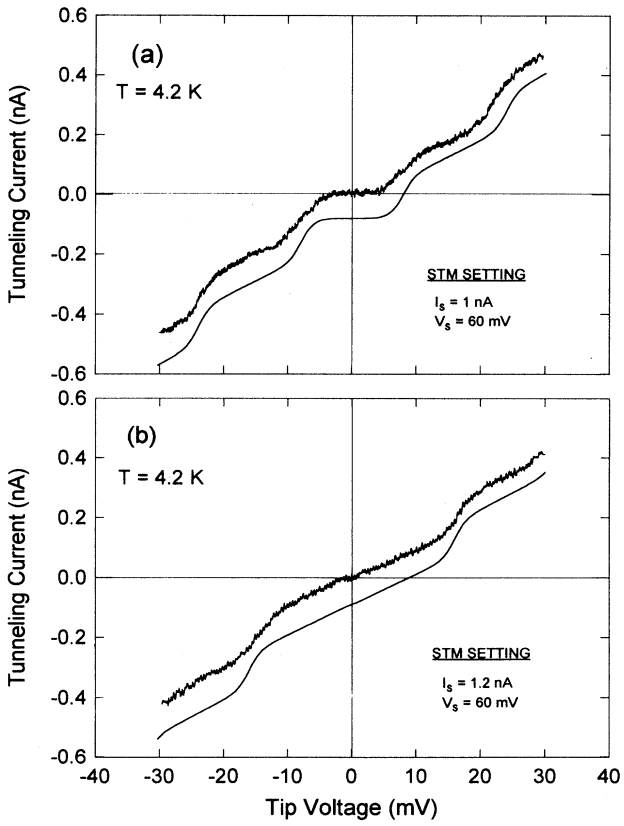

FIG. 4. Two experimental tunneling *I-V* curves ("noisy" lines) measured at 4.2 K at the same lateral position but with different tip-sample separations, determined by the bias and current settings indicated. The corresponding theoretical curves (smooth lines) were calculated from the "orthodox" SET theory, and were shifted for clarity.

which the curves were acquired was *weakly coupled* to its environment, namely, to the neighboring grains and thus to the bulk of the sample. This observation of weak coupling between neighboring grains is consistent with the sharp transition between normal to superconducting behavior, presented above. The fact that no sign of a superconducting-gap structure can be seen in curve (b) suggests that the grain, as well as its environment, were normal. We have also measured, in some places, *I-V* traces which manifest *both* superconductivity and SET effects. These results will be presented in future publications.

In order to account for the data in Fig. 4 we fitted to experiment theoretical curves calculated from the "orthodox" model[9,13] of the double-barrier tunnel junction configuration. The two theoretical curves (smooth lines in Fig. 4) were calculated with the *same* capacitance values, $C_1=1.0\times10^{-17}$ F and $C_2=1.5\times10^{-17}$ F, for the tip-grain and grain-bulk junctions, respectively. We took, however, *different* values for the fractional charge: curve (a) was calculated with $Q_0=0$ and curve (b) with $Q_0=e/2$. The theoretical curves reproduce accurately the experimentally observed steps, as well as the Coulomb blockade in curve (a) and its disappearance in curve (b). One can argue, of course, that, in addition to Q_0, the capacitance C_1, which corresponds to the tip-grain junction, should also be affected upon changing the STM setting. A careful look at the experimental details shows, however, that this change is negligible. Due to the logarithmic dependence of the tip-sample separation on the tunneling current, this separation is not very sensitive to changes in I_S. In our case, where the apparent barrier height was ~2.8 eV, the separation, and therefore the value of C_1, should change by $\sim3\%$ when varying I_S from 1 to 1.2 nA. This change in C_1 ($\sim3\times10^{-19}$ F) is too small to affect significantly the width of the Coulomb blockade and the positions of the staircase steps. However, it is large enough to change Q_0 (mod e) by $e/2$, as can be seen from the expression for Q_0 given above, assuming a work-function difference of the order of one eV.

SUMMARY

We have presented a CSTM study of the local electronic properties of an intermetallic superconductor YNi_2B_2C. The samples were prepared with Ni deficiency in order to ensure a significant presence of a normal phase. Our simultaneous topography and tunneling-spectroscopy measurements have demonstrated a correlation between the spatial variations in the tunneling conductance and in the surface morphology. In particular, we have found that spatial transitions from fully normal to fully superconducting regions occur over distances of ~20 nm. These transitions took place always across grain boundaries observed in the topographic image. The energy gap parameter in the superconducting regions at 4.2 K, as extracted from the tunneling *I-V* curves, was $\Delta=2.55\pm0.05$ meV.

The above results show that our samples constitute a granular superconductor-normal system, where the coupling between neighboring grains is, in many cases, very weak (i.e., large contact resistance between the grains). This granular picture is supported by the fact that in many cases, when the STM tip was situated over nanometer-scale surface grains, the *I-V* characteristics exhibited SET effects. In previous publications[10] we have shown that CSTM is an effective tool for studying the low-temperature local transport properties of granular metal-insulator films. Here we have demonstrated that our studies can be extended to other disordered systems, such as superconductor-normal granular systems.

ACKNOWLEDGMENT

We thank Y. Goldstein for helpful discussions and suggestions.

*To whom correspondence should be addressed.

[1]R. J. Cava, H. Takagi, H. W. Zandbergen, J. J. Krajewski, W. F. Peck, Jr., T. Siegrist, B. Batlogg, R. B. Van Dover, R. J. Fedler, K. Mizuhashi, J. O. Lee, H. Eisaki, and S. Uchida, Nature (London) **367**, 252 (1994).

[2]R. Prozorov, I. Felner, and Y. Yeshurun, Physica C **233**, 367 (1994).

[3]T. Ekino, H. Fujii, M. Kosugi, Y. Zenitani, and J. Akimitzu, Physica C **235-240**, 2529 (1994).

[4]T. Hasagawa, M. Ogino, A. Takagi, E. Watenbe, M. Natoh, H. Takagi, S. Uchida, R. J. Cava, and K. Kitazawa, Physica C **235-240**, 1859 (1994).

[5]T. Siegrist, H. W. Zandbergen, R. J. Cava, J. J. Krajewski, and W. F. Peck, Jr., Nature (London) **367**, 254 (1994).

[6]Q. Chen and K. W. Ng, Phys. Rev. B **45**, 2569 (1992).

[7]J. Appel and D. Fay, Phys. Rev. B **41**, 873 (1990).

[8]R. Kleiner, F. Steinmeyer, G. Kunkel, and P. Muller, Phys. Rev. Lett. **68**, 2349 (1992).

[9]*Single Charge Tunneling, Coulomb Blockade Phenomena in Nanostructures,* edited by H. Grabert and M. H. Devort (Plenum, New York, 1992).

[10]E. Bar-Sadeh, Y. Goldstein, C. Zhang, H. Deng, B. Abeles, and O. Millo, Phys. Rev. B **50**, 8961 (1994); E. Bar-Sadeh, Y. Goldstein, M. Wolovelsky, D. Porath, C. Zhang, H. Deng, B. Abeles, and O. Millo, J. Vac. Sci. Technol. B (to be published).

[11]M. Tinkham, *Introduction to Superconductivity* (Krieger, Malabar, Florida, 1980).

[12]E. L. Wolf, *Principles of Electron Tunneling Spectroscopy* (Oxford University Press, Oxford, 1989).

[13]A. E. Hanna and M. Tinkham, Phys. Rev. B **43**, 5919 (1991).

[14]Z. Y. Rong, A. Chang, L. F. Cohen, and E. L. Wolf, IEEE Trans. Magn. **28**, 67 (1992).

[15]C. Schonenberg, H. van Houten, and H. C. Donkersloot, Europhys. Lett. **20**, 249 (1992).

[16]N. D. Lang, Phys. Rev. B **37**, 10 395 (1988).

[17]A. L. de Lozanne, S. A. Elrod, and C. F. Quate, Phys. Rev. Lett. **54**, 2433 (1985).

[18]A. Chang, Z. Y. Rong, Y. M. Ivanchenko, F. Lu, and E. L. Wolf, Phys. Rev. B **46**, 5692 (1993).

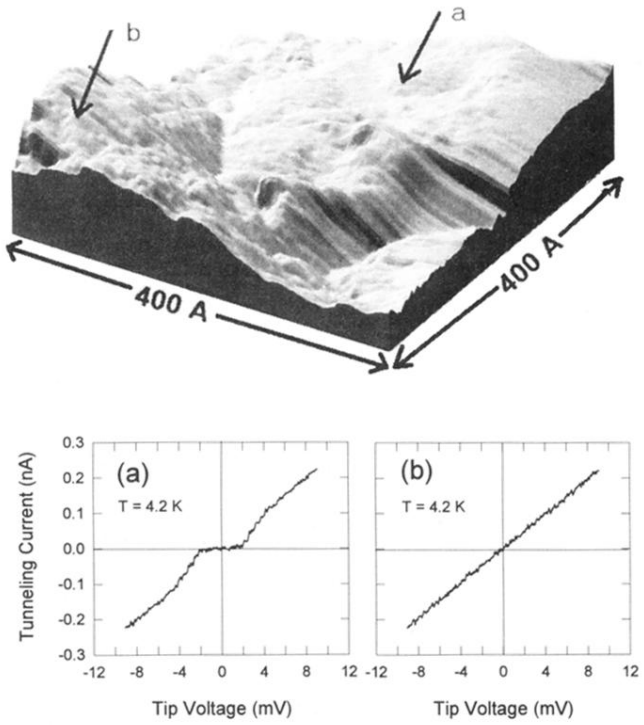

FIG. 3. Topographic image and two tunneling *I-V* characteristics of an YNi_2B_2C sample measured at 4.2 K. Curve (a) was measured in a superconducting region, while curve (b) in a normal region. The tip positions at which the curves were measured are indicated on the topographic image.